Performance Evaluation of a Long-Range RFID Tag Powered by a Vibration Energy Harvester

Yingxian Lu, Philippe Basset, and Jean-Marc Laheurte

***Abstract*—This letter reports the characterization procedure of a radio frequency identification (RFID) tag powered by a microelectromechanical system vibration energy harvester (VEH). The tag antenna and its matching interface to the RFID chip are designed with the help of an electromagnetic simulator. The energy provided by the VEH is stored in a reservoir capacitor and released through a mechanical switch to the tag. It is demonstrated that the tag can communicate with a reader at a distance up to 15 m when powered by the VEH working with an acceleration of 2 g_{rms} and 100 Hz. The energy delivered by the VEH within 100 s can sustain up to six tag readings using the EPC Gen-2 Class-1 standard.**

***Index Terms*—Energy harvesting, impedance matching, semipassive radio frequency identification (RFID) tags.**

I. Introduction

The radio frequency identification (RFID) technology is widely applicable for identification and positioning of objects or persons. The maximum read/write distances of passive RFID tags working at ultrahigh frequency (UHF) in the 860–960-MHz band reach up to 10 m [1] depending on the operating conditions. The long-range performance can be further improved by using battery-assisted tags. However, taking into account the environmental issues of batteries and their limited lifetime, there is a demand to replace the batteries powering active and semipassive RFID tags by energy harvesters, which provide electrical power transduced from the widely existing ambient sources of energy (vibrations, heat, RF, or light) [2].

As the amount of power that can be extracted from the environment is limited, it is practical to store the transduced energy into a reservoir capacitor temporarily. This energy is then released intermittently through an electronic control module (such as an automatic switch) [3] to the RFID chip. The minimum energy requirement for a successful tag reading is related to the average time of a full communication cycle between the reader and one tag.

On the other hand, the energy requirement of the RFID chip for each communication is also related to the chip itself and the capacitor. First, the chip must be connected to a minimum bias voltage to sustain a proper working status. The current and the power consumption of the chip depend on its bias voltage and its input impedance. Second, a minimum period of time is required to perform a full data transmission, during which there is a voltage drop across the capacitor. Finally, the capacitor value is determined through a tradeoff between the amount of ambient power that can be harvested, the available time to power up the tag, the amount of data to be transmitted, and the energy required for it.

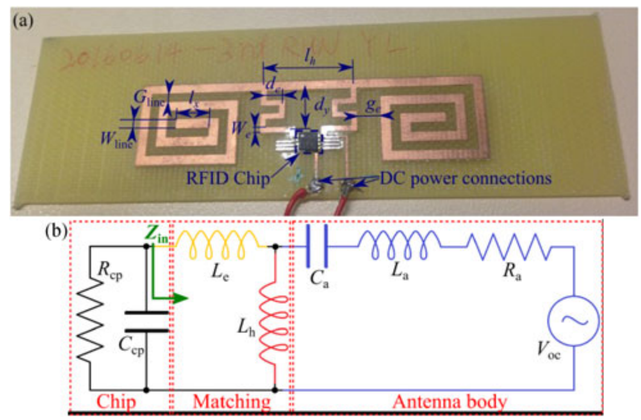

Fig. 1. (a) Photograph of the L-matched RFID tag antenna, including dimensions. (b) Equivalent circuit of the full RFID tag.

In this letter, we describe a new procedure to evaluate the performance of a semipassive UHF RFID tag powered by a capacitive vibration energy harvester (VEH). To the authors' best knowledge, it is the first time that such a study is proposed with a capacitive VEH assisting intermittent communications of an RFID tag, even though a piezoelectric harvester is reported in [4] supporting a continuous tag communication. Our study gives a better understanding of the limitation of VEH-assisted RFID systems under the conditions where the available environmental vibration power is limited.

The key parameters of the tag antenna are first addressed before the impedance of the optimized antenna and the maximum read range (RR) of the tag are measured. Then, the power consumption of the chip biased by a precharged reservoir capacitor is evaluated experimentally, together with the minimum energy requirement for a single reading of the tag. In a following communication experiment, the tag is powered by a capacitor that is charged by a VEH through an ac–dc rectifier. Using a sinusoidal signal to excite a vibrator carrying the VEH, the minimum time and energy requirements of the tag to communicate with the reader are fully determined.

II. Antenna Design: Key Parameters and Simulation

The antenna is based on a spiral-loaded dipole with a modified L-matching circuit interface, the layout of which is

Manuscript received January 13, 2017; accepted March 12, 2017. Date of publication March 15, 2017; date of current version June 26, 2017.

Y. Lu and P. Basset are with the ESYCOM/ESIEE Paris, Université Paris-Est, Noisy-le-Grand Cedex 93162, France (e-mail: yingxian.lu@esiee.fr; p.basset@esiee.fr).

J.-M. Laheurte is with the ESYCOM/UPEM, Université Paris-Est, Champs sur marne 77420, France (e-mail: laheurte@univ-mlv.fr).

Color versions of one or more of the figures in this letter are available online at http://ieeexplore.ieee.org.

Digital Object Identifier 10.1109/LAWP.2017.2682419

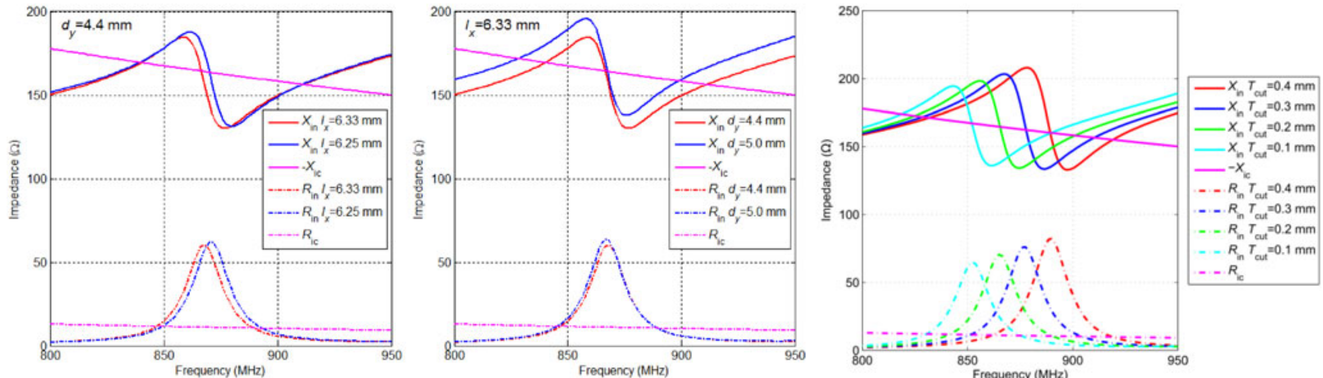

(a) (b) (c)

Fig. 2. Influence of parameters. (a) l_x. (b) d_y. (c) T_{cut} (thickness of the removed substrate material during the milling process) on the design impedance.

shown in Fig. 1(a), together with the illustration of its design parameters. The dipole is loaded by spirals [5], which occupy a much smaller space than meandering lines providing the same amount of inductance. Hence, although the proposed spiral-loaded dipole shows a larger Q-factor for a given resonant frequency than meandering designs [6], it is preferred because of its small size. The dual matching technique described in [7] is applied to reach the largest possible bandwidth for a given dipole. The equivalent circuit of the full tag is shown in Fig. 1(b).

The dipole, the matching circuit, and the chip interface are etched out of a low-cost printed circuit board (PCB) made of FR4 dielectric ($\varepsilon_r = 4.25, \tan\delta = 0.02$, thickness = 1.54 mm) with a 35-μm-thick copper metallization through a milling process. The RFID chip is then soldered on the chip interface.

The chip used is the EM4324 manufactured by EM Microelectronic [8] communicating with the EPC Gen-2 Class-1 protocol and working with the European standard in the 865–868-MHz band. It can be either battery-powered or beam-powered by the RF energy transmitted from a reader. According to the datasheet, the input impedance of the chip at 868 MHz is Z_{ic} = 11-j164 Ω under battery-assisted mode. It is thus equivalent to the impedance of a resistance R_{cp} = 2.456 kΩ in parallel with a capacitor C_{cp} = 7.00 pF. The optimal input impedance of the antenna can be calculated accordingly.

The influences of the different key parameters of the antenna predicted by an ANSYS HFSS model are illustrated in Fig. 2, where the input resistance (R_{in}) and reactance (X_{in}) of the antenna are plotted along with the optimal matching expectations (R_{ic} and $-X_{\mathrm{ic}}$). Here, R_{ic} and X_{ic} are the resistance and the reactance of the chip, respectively, which dependence on frequency is introduced in [1]. As shown in Fig. 2(b), the resonance frequency f_0 of the antenna (the frequency where R_{in} reaches maximum) is reduced by elongating the length of the spiral-loaded dipole (increasing l_x). l_x is thus adjusted so that f_0 is 868 MHz.

Increasing d_y mainly increases X_{in} because it increases the length of the series inductance L_e. Other parameters that have the similar effect as d_y include the meander length (d_e) and the line width (W_e), the increment of which brings an increment of L_e. In contrast, R_{in} is weakly influenced by these parameters.

By adjusting f_0 and X_{in}, the antenna matching can be reached in the largest achievable bandwidth. All the parameters applied

TABLE I
PARAMETERS OF THE ANTENNA DESIGN

Dimension	Value
Line width of dipole and L_h (W_{line})	1.5 mm
Gap between lines (G_{line})	1.5 mm
Length of the innermost segment of the dipoles (l_x)	6.33 mm
Length of L_h (l_h)	14.2 mm
Meander length of L_e (d_e)	3 mm
Line width of L_e (W_e)	0.9 mm
Total height of L_e (d_y)	4.4 mm
Gap between the dipole and L_e (g_e)	3.6 mm

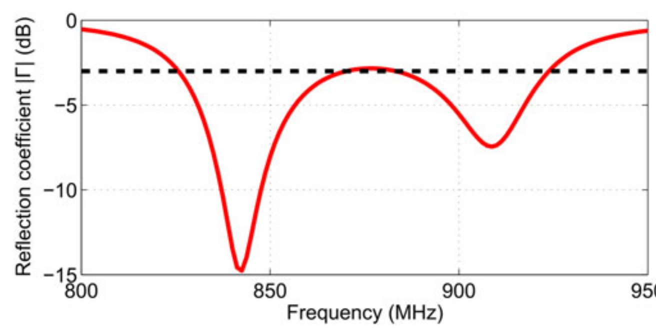

Fig. 3. Reflection coefficient of the tag with parameters listed in Table I.

in the final antenna design are listed in Table I. The reflection coefficient $|\Gamma|$ given by

$$|\Gamma| = \left|\frac{Z_{\mathrm{in}} - Z_{\mathrm{ic}}^*}{Z_{\mathrm{in}} + Z_{\mathrm{ic}}}\right| = \left|\frac{R_{\mathrm{in}} - R_{\mathrm{ic}} + j\,(X_{\mathrm{in}} + X_{\mathrm{ic}})}{R_{\mathrm{in}} + R_{\mathrm{ic}} + j\,(X_{\mathrm{in}} + X_{\mathrm{ic}})}\right| \quad (1)$$

is plotted in Fig. 3. The –3-dB bandwidth of 97 MHz is obtained between 826 and 923 MHz.

The bottleneck in achieving an accurate numerical model is the consideration of the key factors related to the mechanical micromachining process. Among them is T_{cut}, the thickness of substrate material removed by milling, whose influence on the impedance is shown in Fig. 2(c). It appears that a tiny error during the process (even ±0.1 mm) could bring much larger resonance shifts than that of the factor l_x. The cause for this situation is that removing the substrate material that is close to the metal lines reduces the effective permittivity significantly, thus increasing the relative length of the antenna by a large

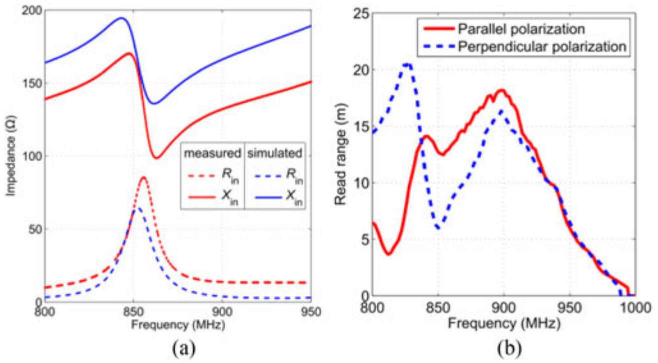

Fig. 4. (a). Input impedance of the antenna (measurement in comparison to simulation). (b). Maximum RR of the RFID tag powered by a 3.3-V battery.

percentage. The measured thickness of removed substrate material is estimated to 0.15 mm with a digital caliper.

III. Experiments and Discussions

A. Antenna Impedance and RR Measurement

The input impedance of the antenna is measured between 800 and 950 MHz using a differential probe measurement technique as stated in [9]. The measured and simulated antenna impedances are shown in Fig. 4(a). The difference between can be attributed in part to the coupling of the dipole near field with the coaxial cable.

The maximum RR of the designed tag is measured with the help of an RFID reader, Tagformance, provided by Voyantic [10]. The reader first measures the minimum transmitted power required to wake up the tag located at a fixed distance. Then, RR is calculated assuming that the maximum allowed power of 2 W is transmitted according to the European regulations. The RFID tag is powered by a 3.3-V battery during the RR measurement. Shown in Fig. 4(b) is the measured RR of the tag, where the main dipole dimension of the tag is either in parallel with or perpendicular to the polarization of the linearly polarized reader antenna. At 868 MHz, RR = 15 m for the parallel polarization. The strong tag response in perpendicular polarization results from the radiation from the orthogonal currents in the spirals.

B. Power Consumption With Capacitive Sources

The power consumption of the RFID tag is measured by biasing the RFID chip with a dc voltage provided by a precharged reservoir capacitor C_{res}. The circuit is shown in the inset of Fig. 5, where the dc input of the chip (R_{chip}) is connected to C_{res}. The distance between the tag and a commercial reader is set just beyond the maximum RR of the batteryless tag (2.5 m). The capacitor is first charged to 3.3 V (maximum supply voltage of the chip). Then, the reader is activated, and repetitive readings of the tag are proceeded. The evolution of voltage V_{res} across C_{res} with time is measured by a voltage follower and recorded until there is no more tag reading, i.e., when V_{res} drops below the supply voltage threshold of 1.1 V.

The power consumption of the tag is determined by calculating the time-derivative of the energy stored in C_{res}

$$P_{\mathrm{chip}} = -\frac{d}{dt}\left[\frac{1}{2}C_{\mathrm{res}}V_{\mathrm{res}}^{2}(t)\right]. \tag{2}$$

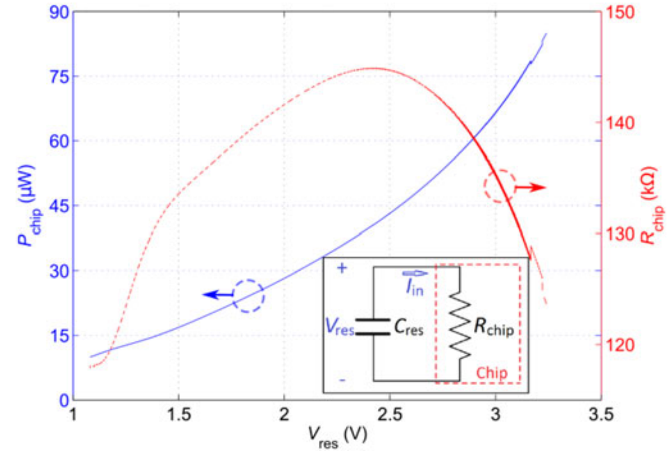

Fig. 5. Power consumption (P_{chip}) and input resistance of the chip (R_{chip}) when powered by a capacitor $C_{\mathrm{res}} = 1$ mF as a function of the bias voltage (V_{res}). The inset shows the experimental schematic.

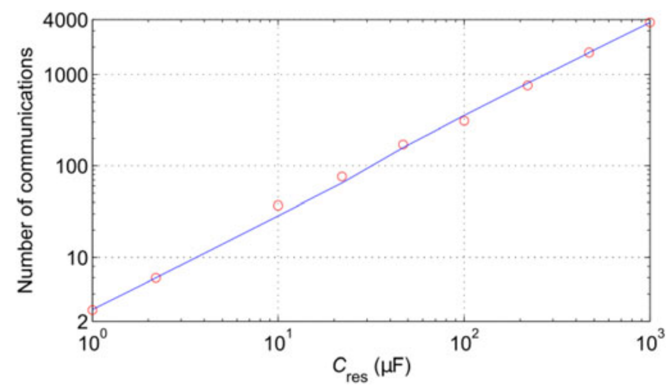

Fig. 6. Number of communications in a row as a function of C_{res} during one full discharge process starting from 3.3 V

The power consumption of the chip (P_{chip}) and its input resistance ($R_{\mathrm{chip}} = V_{\mathrm{res}}^2/P_{\mathrm{chip}}$) together with the current consumption are calculated. When C_{res} varies from 1 to 1 mF, the measured power consumption at given voltages is equivalent, with a relative variation of 10%.

Shown in Fig. 5 are the power consumption and chip resistance as a function of the biasing voltage (V_{res}) measured with $C_{\mathrm{res}} = 1$ mF. We choose to show this result for $C_{\mathrm{res}} = 1$ mF because the largest C_{res} allows the longest discharging time, hence the largest number of sampling points and the highest accuracy. R_{chip} varies between 115 and 146 kΩ, i.e., 130 kΩ with a maximum relative error of ±12%, while the current consumption increases approximately linearly with voltage.

We also obtain the total number of communications in a row when the RFID tag is powered by different C_{res}. The number of communications grows linearly with the increase of storage capacitor, as shown in Fig. 6. When $C_{\mathrm{res}} = 1$ mF, the tag is read 3750 times in a row by the reader during a 2.4-min discharging process from 3.3 to 1.1 V, corresponding to an average time for a single tag reading of 38 ms. With a capacitor of 2.2 μF, up to six tag readings can be proceeded during each discharge starting from 3.3 V. This number of duplicated readings is sufficient to guarantee that at least one successful communication is

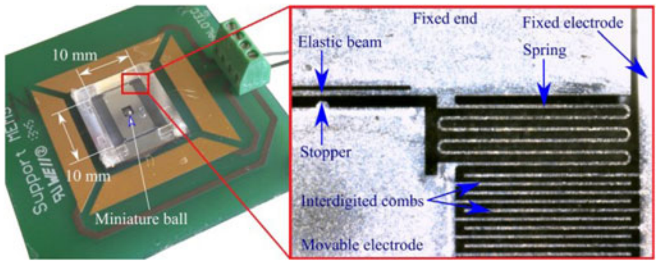

Fig. 7. Macro- and microscale photographs of the VEH assisting the RFID tag.

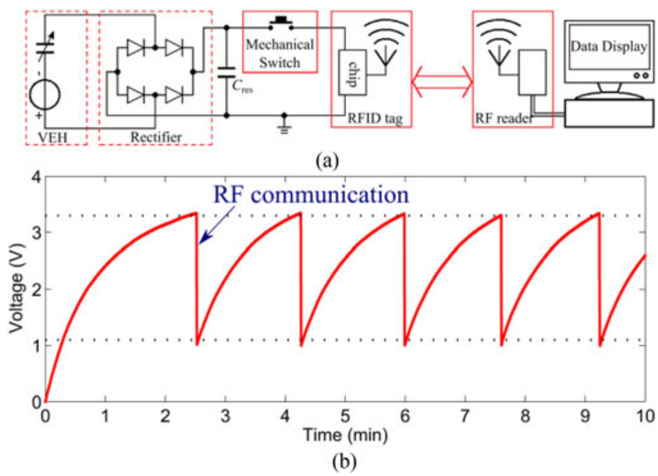

Fig. 8. (a). Schematic of the RFID communication system where the RF tag is powered by a vibration energy harvester. (b) Measured voltage evolution on the bias capacitor C_{res} during the charging and the communication processes.

accomplished in case of any failure. $C_{\mathrm{res}} = 2.2\,\mu$F is thus chosen as the power supply for the RFID tag in the experiment of Section III-C.

C. RF Identification Powered by a MEMS VEH

According to the power consumption measurement, we can conclude that it is possible to power the RFID tag by a $\sim$1-cm^2 microelectromechanical system (MEMS) transducer, i.e., VEH, as proposed in [3]. The transducer (as shown in Fig. 7) is essentially a variable capacitor consisting of gap-closing interdigited combs and biased by a corona-charged electret. It is featured with a wideband resonant structure (spring-mass system) implementing frequency up-conversion mechanisms (miniature ball and elastic stoppers). Working with an optimal resistive load, the VEH can offer up to 2.5 μW with a 2-g_{rms} 100-Hz vibration, providing energy that is capable of supporting several RFID communications within an acceptable duration.

The communication between the tag and the reader is proceeded. The schematic of the experiment is shown in Fig. 8(a), where the reservoir capacitor $C_{\mathrm{res}} = 2.2\,\mu$F is charged by the proposed MEMS VEH through a full-wave diode rectifier. The voltage V_{res} across C_{res} is monitored by a data acquisition card through a high-impedance voltage follower. The energy stored in C_{res} is released by manually pressing a tact switch each time after V_{res} reaches 3.3 V. According to the RC constant of the discharging circuit, V_{res} will drop from the initial voltage to 1.1 V within about 300 ms, after which the current consumption of the chip drops significantly, while there will be no more tag readings. Consequently, the tact switch is released as quickly as possible after being pressed. In a future work, the manually controlled mechanical switch for energy release will be replaced by an automatic Schmitt trigger. The VEH is excited with an acceleration of 2 g_{rms} and 100 Hz. The variation of measured V_{res} is shown in Fig. 8(b). The time required by each charging process from 1.1 to 3.3 V is 100 s. During the capacitor discharge, an average of six tag readings is registered. The average energy consumed by the chip is 1.77 μJ for each tag reading.

IV. Conclusion

In this letter, a full UHF RFID tag powered by a miniature MEMS VEH was designed. The input impedance of the spiral-loaded dipole was optimized with a commercial electromagnetic simulator. The antenna impedance measured with a differential probe method agreed well with the prediction. The high dependence of the antenna impedance on the fabrication process (milling) was pointed out. The maximum RR of the tag reached 15 m at 868 MHz with a 3.3-V battery.

An experimental methodology to evaluate the performance of the VEH-assisted tag was proposed. The first method is to measure the power consumption of the chip when it is biased by a reservoir capacitor, indicating that the number of tag readings is related to the capacitor value. The second method is to use the full VEH-assisted tag, where the energy delivered by the VEH through an ac–dc rectifier is temporarily stored in a 2.2-μF capacitor. With the VEH working at 2 g_{rms} and 100 Hz, an average of six tag readings were observed every 100 s. The average energy consumption of each reading was 1.77 μJ.

In real use-cases, the 100-Hz vibration widely exists as a major multiplication of the industrial frequency, while the 2-g_{rms} accelerations are available on electric motors. The design is thus applicable to the industrial environment. The VEH applied in the system can also respond to even lower frequencies (less than 10 Hz). However, since the power available is proportional to the frequency, the charging duration is inversely proportional to it.

References

[1] J.-M. Laheurte, *UHF RFID Tags: Design and Technologies*. Hoboken, NJ, USA: Wiley, 2014.

[2] N. S. Hudakand and G. Amatucci, “Small-scale energy harvesting through thermoelectric, vibration, and radiofrequency power conversion,” *J. Appl. Phys.*, vol. 103, no. 10, 2008, Art. no. 101301.

[3] Y. Lu, F. Cottone, S. Boisseau, F. Marty, D. Galayko, and P. Basset, “A nonlinear MEMS electrostatic kinetic energy harvester for human-powered biomedical devices,” *Appl. Phys. Lett.*, vol. 107, no. 25, 2015, Art. no. 253902.

[4] A. Hande, R. Bridgelall, and B. Zoghi, “Vibration energy harvesting for disaster asset monitoring using active RFID tags,” *Proc. IEEE*, vol. 98, no. 9, pp. 1620–1628, Sep. 2010.

[5] S. K. Sharma, A. N. Kulkarni, M. R. Thyagarajan, and B. Shanmugam, “A compact spiral loaded planar dipole antenna with frequency reconfiguration,” in *Proc. 2012 IEEE Int. Symp. Antennas Propag.*, 2012, pp. 1–2.

[6] M. Bolic, D. Simplot-Ryl, and I. Stojmenovic, Ed., *RFID Systems: Research Trends and Challenges*. New York, NY, USA: Wiley, 2010, pp. 66–67.

[7] D Deavours, “Analysis and design of wideband passive UHF RFID tags using a circuit model,” in *Proc. Int. Conf. IEEE RFID*, 2009, pp. 283–290.

[8] EM-4324 IC Datasheet, V.7.0, Apr-2015, EM Microelectronic-Marin SA

[9] K. D. Palmer and M. Wvan Rooyen, “Simple broadband measurements of balanced loads using a network analyzer,” *IEEE Trans. Instrum. Meas.*, vol. 55, no. 1, pp. 266–272, Feb. 2006.

[10] Tagformance pro, Voyantic Ltd., Espoo, Finland. [Online]. Available: http://voyantic.com/tagformance_pro